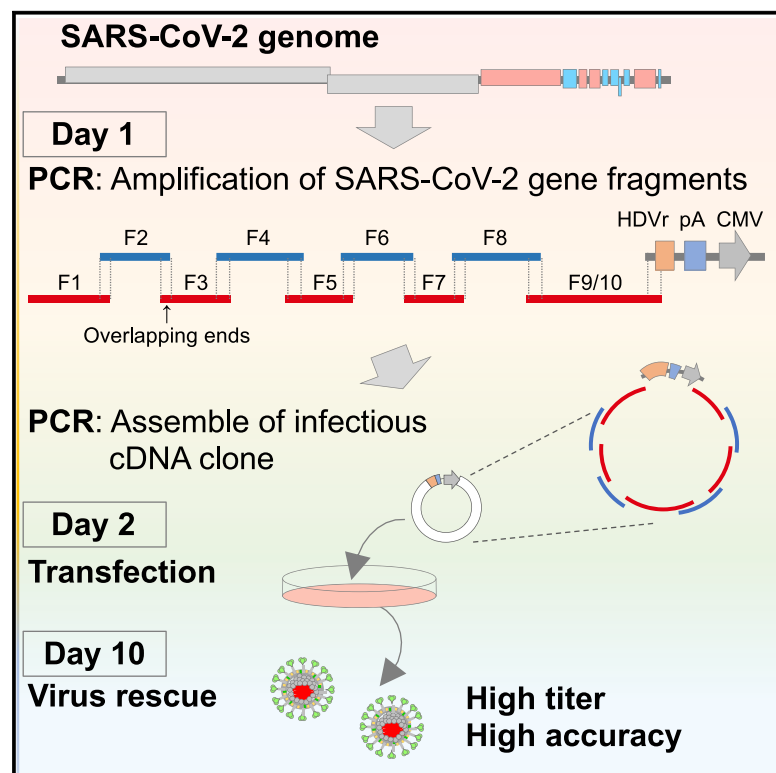# Establishment of a reverse genetics system for SARS-CoV-2 using circular polymerase extension reaction

Graphical abstract

Authors

Shiho Torii, Chikako Ono, Rigel Suzuki, ..., Wataru Kamitani, Takasuke Fukuhara, Yoshiharu Matsuura

Correspondence

fukut@pop.med.hokudai.ac.jp (T.F.), matsuura@biken.osaka-u.ac.jp (Y.M.)

In brief

Torii et al. establish a novel PCR-based, bacterium-free reverse genetics system for SARS-CoV-2 using the CPER method. Recombinant SARS-CoV-2 can be produced with high titers around 2 weeks after amplification of SARS-CoV-2 gene fragments. The method can be applied to generate recombinant SARS-CoV-2 carrying reporter genes or mutations.

Highlights

- A quick PCR-based reverse genetics system is established for SARS-CoV-2

- SARS-CoV-2 recombinants harboring reporter genes or mutations can be generated

Establishment of a reverse genetics system for SARS-CoV-2 using circular polymerase extension reaction

Shiho Torii,[1,4] Chikako Ono,[1,4] Rigel Suzuki,[3] Yuhei Morioka,[1] Itsuki Anzai,[1] Yuzy Fauzyah,[1] Yusuke Maeda,[1] Wataru Kamitani,[2] Takasuke Fukuhara,[3,*] and Yoshiharu Matsuura[1,4,5,*]

[1]Department of Molecular Virology, Research Institute for Microbial Diseases, Osaka University, Suita, Osaka 565-0871, Japan
[2]Department of Infectious Diseases and Host Defense, Graduate School of Medicine, Gunma University, Maebashi, Gunma 371-8511, Japan
[3]Department of Microbiology and Immunology, Graduate School of Medicine, Hokkaido University, Sapporo, Hokkaido 060-8638, Japan
[4]Center for Infectious Diseases Education and Research, Osaka University, Suita, Osaka 565-0871, Japan
[5]Lead contact
*Correspondence: fukut@pop.med.hokudai.ac.jp (T.F.), matsuura@biken.osaka-u.ac.jp (Y.M.)
https://doi.org/10.1016/j.celrep.2021.109014

SUMMARY

Severe acute respiratory syndrome coronavirus 2 (SARS-CoV-2) has been identified as the causative agent of coronavirus disease 2019 (COVID-19). Although multiple mutations have been observed in SARS-CoV-2, functional analysis of each mutation of SARS-CoV-2 has been limited by the lack of convenient mutagenesis methods. In this study, we establish a PCR-based, bacterium-free method to generate SARS-CoV-2 infectious clones. Recombinant SARS-CoV-2 could be rescued at high titer with high accuracy after assembling 10 SARS-CoV-2 cDNA fragments by circular polymerase extension reaction (CPER) and transfection of the resulting circular genome into susceptible cells. The construction of infectious clones for reporter viruses and mutant viruses could be completed in two simple steps: introduction of reporter genes or mutations into the desirable DNA fragments (∼5,000 base pairs) by PCR and assembly of the DNA fragments by CPER. This reverse genetics system may potentially advance further understanding of SARS-CoV-2.

INTRODUCTION

Severe acute respiratory syndrome coronavirus 2 (SARS-CoV-2) in the family *Coronaviridae* is the causative agent of a global pandemic of severe respiratory disease, coronavirus disease 2019 (COVID-19) (Gorbalenya et al., 2020). The virus was initially discovered in Wuhan, China, in late December 2019 (Zhu et al., 2020; Zou et al., 2020; Wu et al., 2020) and has spread worldwide. As of February 2, 2021, more than 100 million COVID-19 cases have been confirmed and more than 2 million deaths have been reported worldwide (https://covid19.who.int/). Various mutations have been accumulated on the genome of SARS-CoV-2 and spread all over the world. For instance, viruses encoding the D614G mutation on the surface of the spike protein (S protein) became predominant (https://nextstrain.org/ncov/global). In addition, human cases infected with the lineage 501Y.V1 and 501Y.V2 viruses have been increasing, in which multiple mutations have been introduced besides D614G (https://nextstrain.org/ncov/global). To understand the function of each mutation in the genes of these viruses, it is essential to generate recombinant virus with each mutation and examine the biological features compared with the parental virus. Although numerous papers have been published since the emergence of SARS-CoV-2, limited studies have generated recombinant SARS-CoV-2 and examined the functions of the viral genes or the molecular mechanisms of the

propagation and pathogenesis of SARS-CoV-2. The development of a simple and efficient reverse genetics system is urgently needed for further molecular studies of SARS-CoV-2.

Although various infectious clones harboring the full-length viral cDNA under suitable promoters in the plasmid have been established, the plasmid system is not available for coronaviruses because of the large size of their viral genomes (−30 kilobases [kb]). Instead, bacterial artificial chromosomes (BACs) or *in vitro* ligation of viral cDNA fragments have been classically used (Almazán et al., 2006; Yount et al., 2003; Scobey et al., 2013; Terada et al., 2019). Although these systems have allowed us to conduct molecular studies of coronaviruses, they have some disadvantages, particularly when performing mutagenesis. In the case of BACs, undesired mutations, such as deletions or insertions, can be introduced during bacterial amplification, and verification of the full-length genome every time is time consuming. Moreover, the *in vitro* ligation method is complicated. Given these facts, it seems difficult to rapidly introduce reporter genes or multiple mutations into viral genes by the classical methods.

Recently, a method for the rapid generation of flavivirus infectious clones by circular polymerase extension reaction (CPER) was reported (Edmonds et al., 2013). In this approach, cDNA fragments covering the full-length viral genome and a linker fragment, which encodes the promoter, poly(A) signal, and ribozyme sequence, are amplified by PCR. Because the amplified
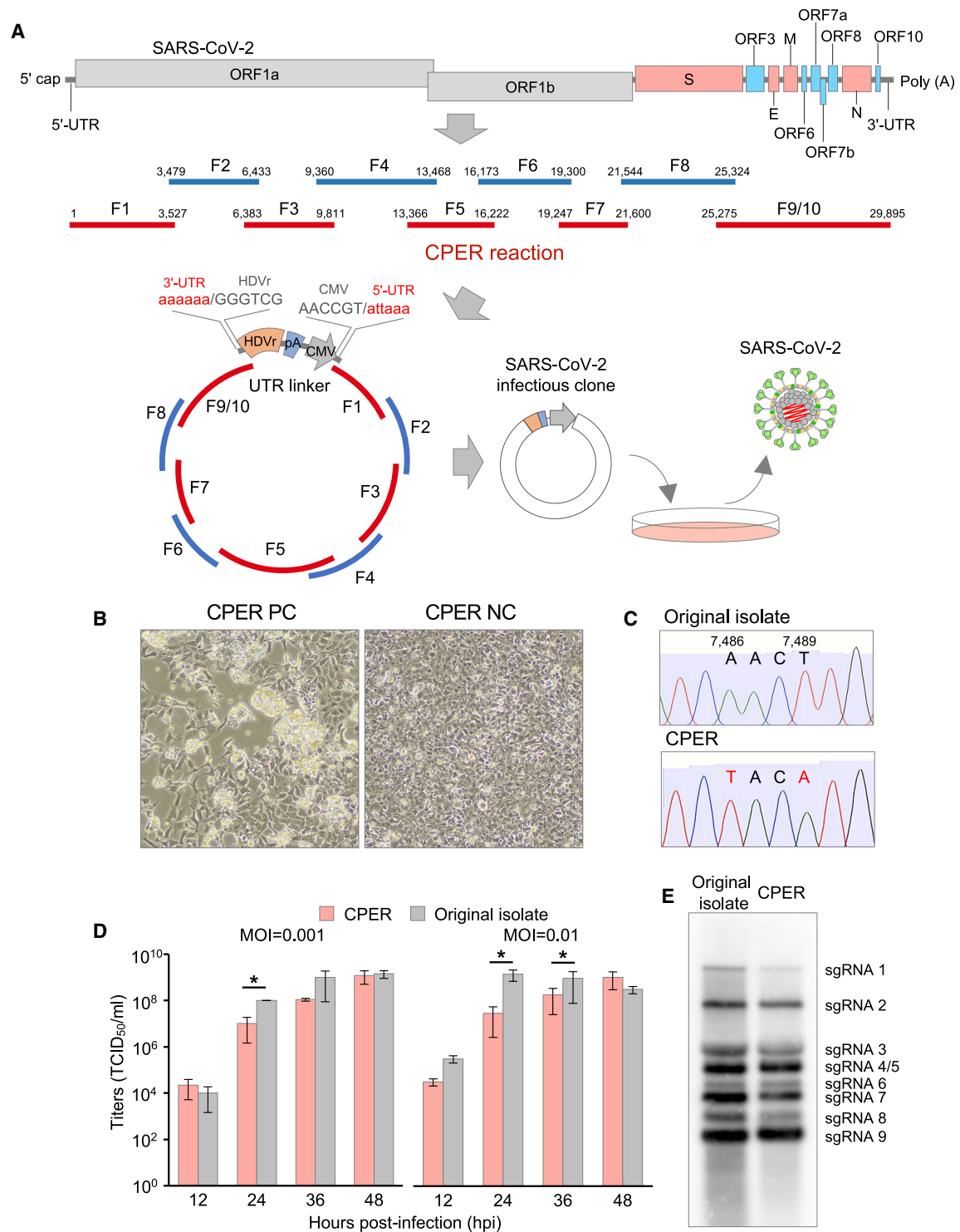
Figure 1. Establishment of CPER-based reverse genetics for SARS-CoV-2

(A) Schematic representation of a CPER approach for the generation of recombinant SARS-CoV-2. A total of 9 fragments covering the full-length of the SARS-CoV-2 genome were amplified and then assembled with a UTR linker fragment by CPER. The resulting CPER products were transfected into the susceptible cells.

(B) HEK293-3P6C33 cells were transfected with the CPER product, and the bright-field image was acquired at 7 dpt (left). As a negative control, the CPER product obtained without fragment F9/10 was transfected into cells, and the image was obtained at 7 dpt (right).

(C) Genetic markers (2 silent mutations, A7486T and T7489A) in the recombinant SARS-CoV-2 genome.

(legend continued on next page)

fragments are designed to include overlapping ends with adjacent fragments, the amplified fragments can be extended as a circular viral genome with a suitable promoter by an additional PCR using the amplified fragments. By direct transfection of the circular viral genome with the promoter into susceptible cells, infectious viruses can be recovered. This means that infectious clones of flaviviruses can be constructed without bacterial amplification or *in vitro* ligation. Using this CPER method, multiple reporter flaviviruses and chimeric flaviviruses have been constructed (Tamura et al., 2018; Piyasena et al., 2019), and various mutant flaviviruses were easily generated and analyzed at the same time (Setoh et al., 2019). These studies showed that CPER is an effective approach for the characterization of viral proteins.

In this study, we tried to establish a CPER method for the construction of SARS-CoV-2 recombinants possessing reporter genes and mutations. In addition, we compared the biological characteristics of the recombinants rescued by the CPER method with the parental SARS-CoV-2.

RESULTS

First, we examined whether the CPER approach would be applicable for the construction of an infectious clone of SARS-CoV-2. For this purpose, we used the SARS-CoV-2 strain SARS-CoV-2/Hu/DP/Kng/19-020, which was provided by Dr. Sakuragi at the Kanagawa Prefectural Institute of Public Health. A total of 10 viral gene fragments (G1 to G10) covering the entire genome of SARS-CoV-2 and a UTR linker fragment encoding the sequences of the 3′ 43 nt of SARS-CoV-2, hepatitis delta virus ribozyme (HDVr), bovine growth hormone (BGH) poly(A) signal, cytomegalovirus (CMV) promoter, and the 5′ 25 nt of SARS-CoV-2 were cloned into plasmids. Then, cDNA fragments of F1 to F10 and the UTR linker, possessing complementary ends with 25 to 452 overlapping nucleotides, were amplified with the specific primers in the Key resources table (CoV-2-F1-Fw to CoV-2-Linker-Rv) and subjected to CPER as templates (Figure 1A). The cDNA fragments of F9 and F10 were connected to F9/10 before CPER by overlap PCR. A negative control was prepared by CPER using cDNA fragments, excluding F9/10. The full-length cDNA clone of SARS-CoV-2 under the CMV promoter obtained by CPER (condition 1 described in STAR Methods) was directly transfected into either BHK-21 cells or tetracycline-inducible ACE2 and TMPRSS-expressing IFNAR1-deficient HEK293 (HEK293-3P6C33) cells without purification steps. Because the SARS-CoV-2 nucleocapsid protein was reported to enhance the propagation of coronavirus RNA transcripts (Xie et al., 2020), the nucleocapsid-expressing plasmid was transfected, together with the CPER products into cells. Upon the induction of ACE2 and TMPRSS expression in HEK293-3P6C33 cells or the overlaying of Vero cells expressing TMPRSS2 (VeroE6/TMPRSS2) onto BHK-21 cells, propagation of SARS-CoV-2 was assessed by cytopathic effects (CPEs).

At 7 days post-transfection (dpt), CPEs were observed in HEK293-3P6C33 cells transfected with the CPER product (CPER PC), but not in those transfected with the negative control (CPER NC) (Figure 1B). CPEs were not observed in BHK-21 cells until 14 dpt of the CPER products (data not shown). Propagation of the progeny viruses was examined by serial passages of the culture supernatants of HEK293-3P6C33 cells in VeroE6/TMPRSS2 cells for 2 rounds. CPEs were observed at 1 day post-infection (dpi) of the viruses of both passage (P) 1 and P2 (data not shown). Infectious titers of the culture supernatants of HEK293-3P6C33 cells at 7 dpt (P0), plus P1 and P2 viruses collected at 2 dpi to VeroE6/TMPRSS2 cells, were determined by 50% tissue culture infective dose ($TCID_{50}$) assays. The infectious titers of the P0, P1, and P2 viruses were $10^{5.8}$, $10^{6.3}$, and $10^{5.8}$ $TCID_{50}$/mL, respectively (data not shown), demonstrating that infectious SARS-CoV-2 was rescued at high titer upon transfection of the CPER product into HEK293-3P6C33 cells and that the recovered viruses were capable of propagating well in VeroE6/TMPRSS2 cells.

To optimize the conditions of recovery of infectious SARS-CoV-2 particles by CPER, the reactions were performed using different numbers of cycles, steps, and extension times (conditions 1 to 3 in STAR Methods). To investigate the effect of expression of nucleocapsid, as shown previously (Xie et al., 2020), on the recovery of infectious particles, CPER products were transfected into HEK293-3P6C33 cells with or without an expression plasmid of the nucleocapsid protein. Culture supernatants of HEK293-3P6C33 cells transfected with the CPER product were collected at the indicated time points for 9 days, and infectious titers were determined as the $TCID_{50}$. In cells transfected with the CPER products without F9/10 (CPER NC), no CPE and no infectious titer in the supernatants was detected until 9 dpt (condition 3 without the expression plasmid of the nucleocapsid protein is shown in Figure S1). However, infectious titers were detected from 5 dpt and reached around $10^{7.0}$ $TCID_{50}$/mL in the supernatants of cells transfected with the CPER products, regardless of the reaction conditions (condition 3 without the expression plasmid of the nucleocapsid protein is shown in Figure S1). No effect of the expression of nucleocapsid protein was observed, suggesting that nucleocapsid is not necessary to recover infectious particles in this method. We selected condition 3 (an initial 2 min of denaturation at 98°C followed by 35 cycles of 10 s at 98°C, 15 s at 55°C, and 15 min at 68°C and a final extension for 15 min at 68°C) for further CPER to generate an infectious cDNA clone for the recovery of infectious particles after transfection into HEK293-3P6C33 cells. Condition 3 was chosen because CPE appeared in cells at 5 dpt of CPER products obtained by condition 3 but at 7 dpt of those obtained by conditions 1 and 2 (data not shown).

To determine the full-length genome sequences of viruses recovered by the CPER method, 2 viruses (1 and 2 in Table 1), which were obtained independently at different time points from the supernatants of HEK293-3P6C33 cells, were subjected

---

(D) Comparison of the growth kinetics of the recombinant SARS-CoV-2 with those of the original isolate. VeroE6/TMPRSS2 cells were infected with the viruses (MOI = 0.001 or 0.01), and infectious titers were determined from 12 to 48 hpi.

(E) Northern blot analyses of subgenomic RNAs. RNAs extracted from cells infected with the parental virus and the recombinant SARS-CoV-2 were subjected to northern blot analyses.

Table 1. Mutations of recombinant SARS-CoV-2

Sample ID	Nucleotide position	Original isolate	CPER recombinant	Region
1	29,687	a	t/a	3' UTR
2	29,687	a	t/a	3' UTR

to Sanger sequence analysis with specific primers. Sequence analyses of viruses demonstrated that the recombinant viruses maintained genetic markers (two silent mutations, A7486T and T7489A; Figure 1C), indicating that there was no contamination of parental virus. Importantly, except for the genetic markers, there was only one difference (T to T/A) in all tested viruses, suggesting that the reverse genetics system for SARS-CoV-2 by CPER had high accuracy.

Next, we investigated the growth kinetics of recombinant viruses in comparison with parental SARS-CoV-2. Recombinant viruses, which were recovered at 7 dpt of CPER products into HEK293-3P6C33 cells, and parental SARS-CoV-2 were infected into VeroE6/TMPRSS2 cells at multiplicities of infection (MOIs) of 0.001 and 0.01, and the infectious titers were determined for 48 h. Although the rescued viruses by CPER exhibited lower titers than the parental viruses (original isolate) at 24 and 36 h post-infection (hpi), no significant difference in maximum titers was observed between the rescued and the parental viruses (Figure 1D). These results suggested that propagation of the rescued SARS-CoV-2 by CPER is slow but reached levels similar to those reached by the parental virus. To examine the viral RNA synthesis of the rescued viruses, northern blot analyses were performed. In total, eight subgenomic RNAs were detected in cells infected with both parental and rescued viruses, and all eight RNAs were similar in size (Figure 1E). Altogether, these results showed that SARS-CoV-2 rescued by the CPER method exhibits *in vitro* biological characteristics similar to those of the parental virus.

Next, we applied the CPER method for construction of recombinant SARS-CoV-2 carrying reporter genes; the workflow of introduction of reporter genes by the CPER method is shown in Figure S2. The nucleotide sequences from 27,433 to 27,675 in open reading frame (ORF) 7 were replaced by the sfGFP gene, as previously reported (Thi Nhu Thao et al., 2020) (Figure 2A). Using the DNA fragments containing the sfGFP gene, infectious DNA clones were assembled by CPER. CPE was observed in HEK293-3P6C33 cells at 7 dpt of the CPER product, and the insertion of the reporter genes in the viruses was confirmed by Sanger sequence analysis (data not shown). Then, the wild-type (WT) virus and sfGFP-carrying virus (GFP virus) were infected into VeroE6/TMPRSS2 cells at an MOI of 0.001, and the growth kinetics of the viruses were evaluated. GFP viruses exhibited lower titers than WT viruses at the indicated time points, and the maximum titers of GFP viruses at 36 hpi were significantly lower than those of WT viruses at 48 hpi (Figure 2B). We also examined the expression of GFP in Vero/TMPRSS2 cells upon infection with the GFP recombinant from 12 to 36 hpi by fluorescence microscopy. The numbers of GFP-positive cells were increased from 12 to 36 hpi, and almost all cells exhibited the fluorescent signals at 24 and 36 hpi (Fig-

ure 2C). To examine the stability of the sfGFP gene, we serially passaged GFP viruses in VeroE6/TMPRSS2 cells five times (P1–P5). During five-time passage, sfGFP genes were maintained in GFP viruses without mutations (data not shown), and GFP signals were detected in VeroE6/TMPRSS2 cells at 24 hpi with GFP viruses (P1 to P5) at an MOI of 0.01 (Figure S3A). These results indicate that recombinant SARS-CoV-2 harboring reporter genes could be quickly engineered by the CPER method and the sfGFP gene in the ORF7a was stable in the SARS-CoV-2 genome.

We also employed NanoLuc binary technology (NanoBiT) (Dixon et al., 2016). NanoBiT is a split reporter consisting of 2 subunits: high-affinity NanoBiT (HiBiT) (Schwinn et al., 2018) and large NanoBiT (LgBiT). By interaction of HiBiT and LgBiT, NanoLuc enzymatic activity can be detected. Because a reporter virus can be generated by inserting a small cDNA fragment encoding 11 amino acids into the viral genome, the effect on viral growth and pathogenicity has been shown to be minimal (Tamura et al., 2018). In this study, we inserted a HiBiT luciferase gene (VSGWRLFKKIS) and a linker sequence (GSSG) into the N terminus of the ORF6 gene of SARS-CoV-2 (Figure 2A) by overlap PCR using DNA fragment F9 and specific primer sets (see STAR Methods for details), and the recombinant SARS-CoV-2 possessing HiBiT was generated by CPER using the resulting fragments (Figure S2). We confirmed the incorporation of the HiBiT gene into the recombinant viruses by Sanger sequence analysis (data not shown). Infectious titers of the HiBiT recombinants (ORF6-HiBiT) were comparable to those of the WT (Figure 2D). Luciferase activities in cells infected with the recombinant viruses, as assessed by addition of LgBiT protein into the cell lysates, were increased from 12 to 48 hpi (Figure 2E). The stability of the HiBiT gene in the N terminus of ORF6 was examined by five-time passages of the HiBiT viruses. The HiBiT luciferase gene was maintained at least up to P5 (Figure S3B). In addition, similar luciferase activities were detected in cells at 24 hpi with HiBiT viruses at an MOI of 0.01 (Figure S3C). These results suggest that recombinant SARS-CoV-2 carrying HiBiT could be easily generated by the CPER method and HiBiT viruses exhibited growth kinetics similar to those of WT virus and stability of the HiBiT gene in the SARS-CoV-2 genome.

Finally, we examined whether the CPER method can be applied for the construction of recombinant SARS-CoV-2 with the desired mutations. Substitution of D614 to G on the S protein was frequently detected and became dominant in European, South American, and North American countries (Koyama et al., 2020) (https://nextstrain.org/ncov/global). To evaluate the effect of this substitution on virus propagation, we introduced this mutation in fragment F8 of SARS-CoV-2 (strain SARS-CoV-2/Hu/DP/Kng/19-020) by overlap PCR and generated the infectious clone by the CPER method (Figure S2). We confirmed the substitution in the recombinant by Sanger sequence analysis (data not shown), but there was no difference in growth kinetics between the WT and the D614G recombinant in VeroE6/TMPRSS2 cells (Figure 2F). Collectively, these results suggest that our novel reverse genetics system based on CPER is an efficient method for quick generation of recombinants for SARS-CoV-2.
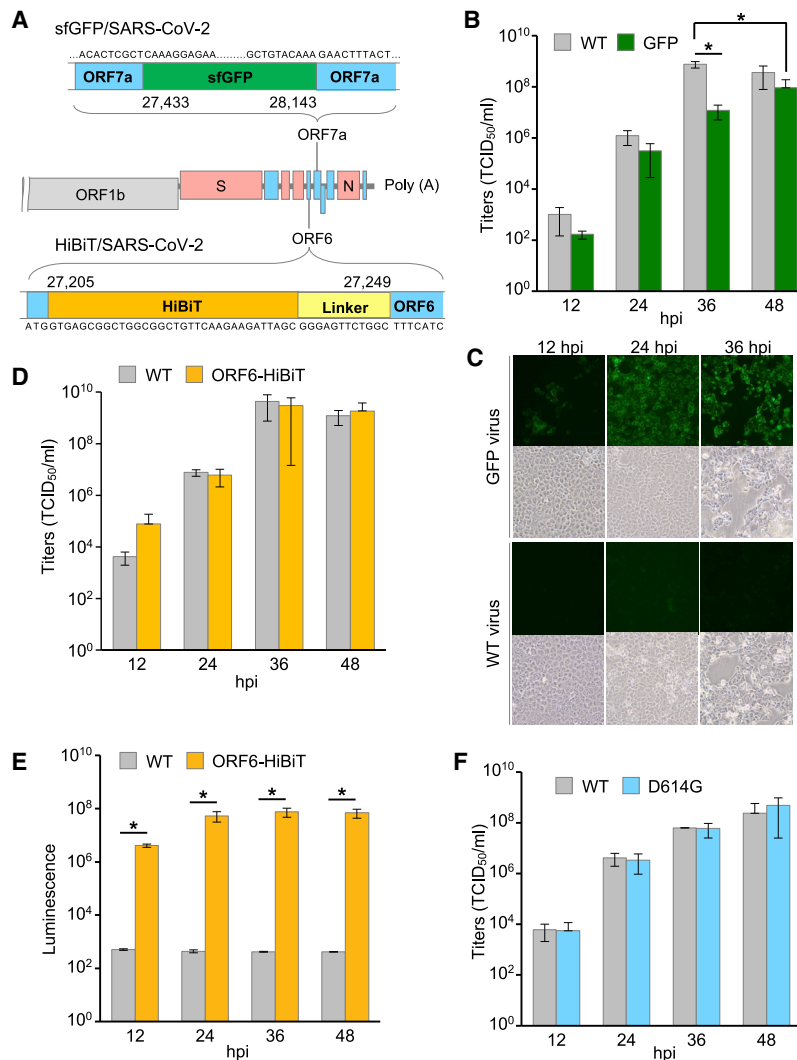
Figure 2. Characterization of SARS-CoV-2 recombinants possessing reporter genes and mutations

(A) Gene structure of recombinant SARS-CoV-2 carrying the sfGFP or HiBiT gene.

(B) Growth kinetics of wild-type SARS-CoV-2 (WT) and SARS-CoV-2 carrying sfGFP (GFP). VeroE6/TMPRSS2 cells were infected with the viruses (MOI = 0.001), and infectious titers were determined at the indicated time points.

(C) Fluorescent signal in VeroE6/TMPRSS2 cells infected with the WT virus and GFP virus was observed for 36 hpi.

(D) Growth kinetics of the WT virus and recombinant virus possessing the HiBiT gene in ORF6 (ORF6-HiBiT). Titers in the culture supernatants of VeroE6/TMPRSS2 cells, infected with the viruses (MOI = 0.01), were measured for 48 h.

(E) Luciferase activities in VeroE6/TMPRSS2 cells infected with the WT virus and ORF6-HiBiT virus were determined from 12 to 48 hpi.

(F) Infectious titers of the WT virus or mutant virus, harboring a substitution of D614 to G in the spike protein (D614G), were determined at the indicated time points.

the function of viral genes and the mechanisms of propagation and pathogenesis.

In this study, we first report that the CPER method is available to assemble a large genome (30 kb) of SARS-CoV-2 with high accuracy. Although infectious clones were recovered by all CPER conditions we examined, recombinant viruses were recovered only in HEK293-3P6C33 cells (Figure 1B), indicating that the transfection efficiency of the CPER product and replication efficiency of viruses might be important to produce recombinant viruses. Multiple primer sets for the generation of DNA fragments (F1–F10) were examined (data not shown); however, recombinant viruses were recovered only when using the fragments generated by the indicated primer sets. Because each SARS-CoV-2 subgenomic RNA contains a common leader sequence (72 nucleotides) at the 5′ end (Kim et al., 2020), the design of optimal primer sets seemed to be important for efficient assembly of the circular genome. In the case of the CPER method for flaviviruses, it was reported that insect-specific flaviviruses, which can replicate only in insect-derived cells, could be rescued using mosquito-derived C6/36 cells by replacing the CMV promoter with the modified OpIE2 promoter gene in the UTR linker fragment (Piyasena et al., 2017). In that sense, further investigation of the CPER conditions (i.e., promoter sequences and primer sets) for SARS-CoV-2 may enhance the recovery of recombinants, even for slowly growing viruses. Moreover, it might be possible to generate other coronaviruses and chimeric coronaviruses using susceptible cell lines and optimal promoters.

The growth of rescued SARS-CoV-2 by CPER was slow compared with the parental virus, consistent with the previous report (Xie et al., 2020). It was thought that a recombinant virus was generated from a single cDNA clone and possesses less

DISCUSSION

Reverse genetics is one of the essential tools to analyze the functions of viral genes; however, because of the large size of the coronavirus genome, gene manipulations for coronaviruses have been performed by only a limited number of groups. Here, we established a simple and quick reverse genetics system for SARS-CoV-2 based on the CPER method. This system consists of two steps—namely, amplification of fragments encoding promoter and viral genes followed by assembly into infectious cDNA clones by PCR (CPER) without bacterial amplification or *in vitro* transcription. Recombinant viruses were generated with high titers at 7 dpt of CPER products into cells. Using high-fidelity polymerase, SARS-CoV-2 could be rescued with high accuracy, and the rescued virus exhibited characteristics similar to those of the parental virus. The same tools, i.e., primers and promoter fragments, can be used for generation of viruses possessing multiple mutations or reporters. This method will allow us to conduct high-throughput mutagenesis of SARS-CoV-2 to clarify

fitness to hosts, whereas a parental SARS-CoV-2 possesses high fitness to hosts because it can maintain more heterologous clones. The GFP recombinant virus exhibited a lower titer than the WT viruses, but the HiBiT recombinants exhibited growth kinetics similar to those of the WT virus, suggesting that the small HiBiT gene has little effect to virus propagation and the HiBiT virus might be suitable for functional analyses. As we showed previously, HiBiT recombinant viruses could be useful for drug screening and animal experiments (Tamura et al., 2018, 2019). By combining the reporter assay and mutational scanning, we are able to investigate the biological features of viral genes of SARS-CoV-2.

To characterize escape mutants emerging through the use of antiviral drugs or vaccinations, CPER can be a robust tool. By the CPER method, it might be feasible to generate an avirulent strain for use as a safe live-attenuated vaccine for SARS-CoV-2. In addition to classical reverse genetics systems for coronaviruses, our method will broaden the options for coronavirus genetic manipulation systems. We believe that the CPER method described in this study will be widely used to investigate the molecular mechanisms of the proliferation and pathogenesis of SARS-CoV-2.

STAR★METHODS

Detailed methods are provided in the online version of this paper and include the following:

- KEY RESOURCES TABLE
- RESOURCE AVAILABILITY
  - Lead contact
  - Materials availability
  - Data code and availability
- EXPERIMENTAL MODEL AND SUBJECT DETAILS
- METHOD DETAILS
  - RNA extraction, cDNA synthesis, and determination of nucleotide sequences of the full-length SARS-CoV-2 genome
  - Plasmids
  - CPER reaction
  - Transfection
  - Titration and growth kinetics
  - Northern blotting
  - HiBiT luciferase assay
- QUANTIFICATION AND STATISTICAL ANALYSIS

AUTHOR CONTRIBUTIONS

S.T. performed all experiments and analyzed the data under the supervision of T.F. and Y. Matsuura; C.O., R.S., Y. Morioka, I.A., Y.F., W.K., and Y. Maeda provided critical resources and scientific insights; S.T. and T.F. wrote the original draft; and C.O., R.S., Y. Morioka, I.A., Y.F., W.K., Y. Maeda, and Y. Matsuura wrote, reviewed, and edited the final manuscript.

REFERENCES

Almazán, F., Dediego, M.L., Galán, C., Escors, D., Alvarez, E., Ortego, J., Sola, I., Zuñiga, S., Alonso, S., Moreno, J.L., et al. (2006). Construction of a severe acute respiratory syndrome coronavirus infectious cDNA clone and a replicon to study coronavirus RNA synthesis. J. Virol. 80, 10900–10906.

Dixon, A.S., Schwinn, M.K., Hall, M.P., Zimmerman, K., Otto, P., Lubben, T.H., Butler, B.L., Binkowski, B.F., Machleidt, T., Kirkland, T.A., et al. (2016). NanoLuc Complementation Reporter Optimized for Accurate Measurement of Protein Interactions in Cells. ACS Chem. Biol. 11, 400–408.

Edmonds, J., van Grinsven, E., Prow, N., Bosco-Lauth, A., Brault, A.C., Bowen, R.A., Hall, R.A., and Khromykh, A.A. (2013). A novel bacterium-free method for generation of flavivirus infectious DNA by circular polymerase extension reaction allows accurate recapitulation of viral heterogeneity. J. Virol. 87, 2367–2372.

Gorbalenya, A.E., Baker, S.C., Baric, R.S., de Groot, R.J., Drosten, C., Gulyaeva, A.A., Haagmans, B.L., Lauber, C., Leontovich, A.M., Neuman, B.W., et al.; Coronaviridae Study Group of the International Committee on Taxonomy of Viruses (2020). The species Severe acute respiratory syndrome-related coronavirus: classifying 2019-nCoV and naming it SARS-CoV-2. Nat. Microbiol. 5, 536–544.

Kim, D., Lee, J.Y., Yang, J.S., Kim, J.W., Kim, V.N., and Chang, H. (2020). The Architecture of SARS-CoV-2 Transcriptome. Cell 181, 914–921.e10.

Koyama, T., Weeraratne, D., Snowdon, J.L., and Parida, L. (2020). Emergence of Drift Variants That May Affect COVID-19 Vaccine Development and Antibody Treatment. Pathogens 9, 324.

Li, Z., Yu, M., Zhang, H., Wang, H.Y., and Wang, L.F. (2005). Improved rapid amplification of cDNA ends (RACE) for mapping both the 5′ and 3′ terminal sequences of paramyxovirus genomes. J. Virol. Methods 130, 154–156.

Piyasena, T.B.H., Setoh, Y.X., Hobson-Peters, J., Newton, N.D., Bielefeldt-Ohmann, H., McLean, B.J., Vet, L.J., Khromykh, A.A., and Hall, R.A. (2017). Infectious DNAs derived from insect-specific flavivirus genomes enable identification of pre- and post-entry host restrictions in vertebrate cells. Sci. Rep. 7, 2940.

Piyasena, T.B.H., Newton, N.D., Hobson-Peters, J., Vet, L.J., Setoh, Y.X., Bielefeldt-Ohmann, H., Khromykh, A.A., and Hall, R.A. (2019). Chimeric viruses of the insect-specific flavivirus Palm Creek with structural proteins of vertebrate-infecting flaviviruses identify barriers to replication of insect-specific flaviviruses in vertebrate cells. J. Gen. Virol. 100, 1580–1586.

Schwinn, M.K., Machleidt, T., Zimmerman, K., Eggers, C.T., Dixon, A.S., Hurst, R., Hall, M.P., Encell, L.P., Binkowski, B.F., and Wood, K.V. (2018). CRISPR-Mediated Tagging of Endogenous Proteins with a Luminescent Peptide. ACS Chem. Biol. 13, 467–474.

Scobey, T., Yount, B.L., Sims, A.C., Donaldson, E.F., Agnihothram, S.S., Menachery, V.D., Graham, R.L., Swanstrom, J., Bove, P.F., Kim, J.D., et al. (2013). Reverse genetics with a full-length infectious cDNA of the Middle East respiratory syndrome coronavirus. Proc. Natl. Acad. Sci. USA *110*, 16157–16162.

Setoh, Y.X., Prow, N.A., Peng, N., Hugo, L.E., Devine, G., Hazlewood, J.E., Suhrbier, A., and Khromykh, A.A. (2017). *De Novo* Generation and Characterization of New Zika Virus Isolate Using Sequence Data from a Microcephaly Case. MSphere *2*, e00190-17.

Setoh, Y.X., Amarilla, A.A., Peng, N.Y.G., Griffiths, R.E., Carrera, J., Freney, M.E., Nakayama, E., Ogawa, S., Watterson, D., Modhiran, N., et al. (2019). Determinants of Zika virus host tropism uncovered by deep mutational scanning. Nat. Microbiol. *4*, 876–887.

Tamura, T., Fukuhara, T., Uchida, T., Ono, C., Mori, H., Sato, A., Fauzyah, Y., Okamoto, T., Kurosu, T., Setoh, Y.X., et al. (2018). Characterization of Recombinant Flaviviridae Viruses Possessing a Small Reporter Tag. J. Virol. *92*, e01582-17.

Tamura, T., Igarashi, M., Enkhbold, B., Suzuki, T., Okamatsu, M., Ono, C., Mori, H., Izumi, T., Sato, A., Fauzyah, Y., et al. (2019). *In Vivo* Dynamics of Reporter *Flaviviridae* Viruses. J. Virol. *93*, e01191-19.

Terada, Y., Kuroda, Y., Morikawa, S., Matsuura, Y., Maeda, K., and Kamitani, W. (2019). Establishment of a Virulent Full-Length cDNA Clone for Type I Feline Coronavirus Strain C3663. J. Virol. *93*, e01208-19.

Thi Nhu Thao, T., Labroussaa, F., Ebert, N., V'kovski, P., Stalder, H., Portmann, J., Kelly, J., Steiner, S., Holwerda, M., Kratzel, A., et al. (2020). Rapid reconstruction of SARS-CoV-2 using a synthetic genomics platform. Nature *582*, 561–565.

Wu, F., Zhao, S., Yu, B., Chen, Y.M., Wang, W., Song, Z.G., Hu, Y., Tao, Z.W., Tian, J.H., Pei, Y.Y., et al. (2020). A new coronavirus associated with human respiratory disease in China. Nature *579*, 265–269.

Xie, X., Muruato, A., Lokugamage, K.G., Narayanan, K., Zhang, X., Zou, J., Liu, J., Schindewolf, C., Bopp, N.E., Aguilar, P.V., et al. (2020). An Infectious cDNA Clone of SARS-CoV-2. Cell Host Microbe *27*, 841–848.e3.

Yount, B., Curtis, K.M., Fritz, E.A., Hensley, L.E., Jahrling, P.B., Prentice, E., Denison, M.R., Geisbert, T.W., and Baric, R.S. (2003). Reverse genetics with a full-length infectious cDNA of severe acute respiratory syndrome coronavirus. Proc. Natl. Acad. Sci. USA *100*, 12995–13000.

Yusa, K., Rad, R., Takeda, J., and Bradley, A. (2009). Generation of transgene-free induced pluripotent mouse stem cells by the piggyBac transposon. Nat. Methods *6*, 363–369.

Yusa, K., Zhou, L., Li, M.A., Bradley, A., and Craig, N.L. (2011). A hyperactive piggyBac transposase for mammalian applications. Proc. Natl. Acad. Sci. USA *108*, 1531–1536.

Zhu, N., Zhang, D., Wang, W., Li, X., Yang, B., Song, J., Zhao, X., Huang, B., Shi, W., Lu, R., et al.; China Novel Coronavirus Investigating and Research Team (2020). A Novel Coronavirus from Patients with Pneumonia in China, 2019. N. Engl. J. Med. *382*, 727–733.

Zou, L., Ruan, F., Huang, M., Liang, L., Huang, H., Hong, Z., Yu, J., Kang, M., Song, Y., Xia, J., et al. (2020). SARS-CoV-2 Viral Load in Upper Respiratory Specimens of Infected Patients. N. Engl. J. Med. *382*, 1177–1179.

STAR★METHODS

KEY RESOURCES TABLE

REAGENT or RESOURCE	SOURCE	IDENTIFIER
Bacterial and virus strains		
SARS-CoV-2/Hu/DP/Kng/19-020	Kanagawa Prefectural Institute of Public Health	N/A
Escherichia coli DH5-α	New England Biolabs	Cat#C2987
Chemicals, peptides, and recombinant proteins		
100 unit/ml penicillin and 100 μg/ml streptomycin (P/S)	Sigma	Cat#09367-34
G418	Nacalai Tesque	Cat#09380-44
Blasticidin solution	InvivoGen	Cat#ant-bl
Doxycycline hydrochloride	Sigma	Cat#D3447-500MG
Trans IT LT-1	Mirus	Cat#MIR2306
PureLink RNA Mini Kit	Thermo Fisher Scientific	Cat#12183025
PrimeScript RT reagent kit (Perfect Real Time)	TaKaRa Bio	Cat#RR037A-3
PrimeSTAR GXL DNA polymerase	TaKaRa Bio	Cat#R050A
5′RACE System for Rapid Amplification of cDNA Ends, Version 2.0	Thermo Fisher Scientific	Cat#18374-041
DIG RNA Labeling kit (SP6/T7)	Roche	Cat#1175025910
DIG wash and block buffer set	Roche	Cat#11585762001
CDP-Star Chemiluminescent substrate	Sigma	Cat#c0721-100ml
Nano-Glo HiBiT Lytic detection system	Promega	Cat#N3030
Experimental models: Cell lines		
Vero E6 cells	American Type Culture Collection	CRL-1586
BHK-21 cells	Japanese Collection of Research Bioresources Cell Bank	JCRB9020
TMPRSS2-expressing Vero E6 cells	Japanese Collection of Research Bioresources Cell Bank	JCRB1819
Tetracycline-inducible ACE2 and TMPRSS-expressing IFNAR1-deficient HEK293 (HEK293-3P6C33) cells	This paper	N/A
Oligonucleotides		
CoV-2-G1-Fw (attaaaggtttataccttcccaggtaa caaaccaaccaactttcgatctc)	Fasmac	N/A
CoV-2-G1-Rv (tctacacaaactcttaa agaatgtataggg)	Fasmac	N/A
CoV-2-G2-Fw (cggcagtgaggacaatcagacaactac)	Fasmac	N/A
CoV-2-G2-Rv (ggcttagcataattagctatagtatcccaagggac)	Fasmac	N/A
CoV-2-G3-Fw (gccacgtataaaccaaatacctggtgtatacg)	Fasmac	N/A
CoV-2-G3-Rv (ggtgcacagcgcagcttcttcaaaagtactaaagg)	Fasmac	N/A
CoV-2-G4-Fw (agtggtagatgggtacttaacaatgattattac)	Fasmac	N/A
CoV-2-G4-Rv (gtttaaaaacgattgtgcatcagctgactg)	Fasmac	N/A
CoV-2-G5-Fw (acaacctaaatagaggtatggtacttggtag)	Fasmac	N/A
CoV-2-G5-Rv (gtggtttatgtgatttacaataatagctc)	Fasmac	N/A
CoV-2-G6-Fw (tgtagatgatatcgtaaaaacagatggtacac)	Fasmac	N/A
CoV-2-G6-Rv (aacgtgttatacacgtagcagactttagtggtac)	Fasmac	N/A
CoV-2-G7-Fw (aaaggttcaacacatggttgttaaagctgc)	Fasmac	N/A
CoV-2-G7-Rv (cgtacactttgtttctgagagagggtc)	Fasmac	N/A
CoV-2-G8-Fw (atgtttgtttttcttgtttattgccactag)	Fasmac	N/A
CoV-2-G8-Rv (aagttcgtttatgtgtaatgtaatttgactcc)	Fasmac	N/A

(Continued on next page)

Continued

REAGENT or RESOURCE	SOURCE	IDENTIFIER
CoV-2-G9-Fw (gaaccacaaatcattactacagacaacac)	Fasmac	N/A
CoV-2-G9-Rv (gttcgtttaggcgtgacaagtttcattatg)	Fasmac	N/A
CoV-2-G10-Fw (atgtttcatctcgttgactttcaggttactatag)	Fasmac	N/A
CoV-2-G10-Rv (tttttttttttttttttttttttttttgtcattctcc)	Fasmac	N/A
CoV-2-Race1 (gctgatgatcggctgcaacacggacg)	Fasmac	N/A
CoV-2-Race2 (gccacacagattttaaagttcgtttagag)	Fasmac	N/A
CoV-2-F1-Fw (CTATATAAGCAGAGCTCGTTTAGTGA ACCGTattaaaggtttataccttcccaggtaac)	Fasmac	N/A
CoV-2-F1-Rv (cagattcaacttgcatggcattgttagtagccttatttaaggctcctgc)	Fasmac	N/A
CoV-2-F2-Fw (gcaggagccttaaataaggctactaacaatgccatgcaagttgaatctg)	Fasmac	N/A
CoV-2-F2-Rv (ggtaggattttccactacttcttcagagactggttttagatcttcgcaggc)	Fasmac	N/A
CoV-2-F3-Fw (gcctgcgaagatctaaaaccagtctctgaagaagtagtggaaaatcctacc)	Fasmac	N/A
CoV-2-F3-Rv (ggtgcacagcgcagcttcttcaaaagtactaaagg)	Fasmac	N/A
CoV-2-F4-Fw (caccactaattcaacctattggtgctttggacatatcagcatctatagtagctggtgg)	Fasmac	N/A
CoV-2-F4-Rv (gtttaaaaacgattgtgcatcagctgactg)	Fasmac	N/A
CoV-2-F5-Fw (cacagtctgtaccgtctgcggtatgtggaaaggttatggctgtagttgtgatc)	Fasmac	N/A
CoV-2-F5-Rv (gcggtgtgtacatagcctcataaaactcaggttcccaataccttgaagtg)	Fasmac	N/A
CoV-2-F6-Fw (cacttcaaggtattgggaacctgagttttatgaggctatgtacacaccgc)	Fasmac	N/A
CoV-2-F6-Rv (catacaaactgccaccatcacaaccaggcaagttaaggttagatagcactctag)	Fasmac	N/A
CoV-2-F7-Fw (ctagagtgctatctaaccttaacttgcctggttgtgatggtggcagtttgtatg)	Fasmac	N/A
CoV-2-F7-Rv (ctagagactagtggcaataaaacaagaaaaacaaacattgttcgtttagttgttaac)	Fasmac	N/A
CoV-2-F8-Fw (gttaacaactaaacgaacaatgtttgttttcttgttttattgccactagtctctag)	Fasmac	N/A
CoV-2-F8-Rv (gcagcaggatccacaagaacaacagcccttgagacaactacagcaactgg)	Fasmac	N/A
CoV-2-F9-Fw (ccagttgctgtagttgtctcaagggctgttgttcttgtggatcctgctgc)	Fasmac	N/A
CoV-2-F9-Rv (caatctccattggttgctcttcatc)	Fasmac	N/A
CoV-2-F10-Fw (gatgaagagcaaccaatggagattg)	Fasmac	N/A
CoV-2-F10-Rv (GGAGATGCCATGCCGACC Ctttttttttttttttttttttttttttgtcattctcctaag)	Fasmac	N/A
CoV-2-Linker-Fw (cttaggagaatgacaaaaaaaaaaaa aaaaaaaaaaaaaGGGTCGGCATGGCATCTCC)	Fasmac	N/A
CoV-2-Linker-Rv (gttacctgggaaggtataaacctttaatA CGGTTCACTAAACGAGCTCTGCTTATATAG)	Fasmac	N/A
ORF6-HiBiT-Rv (ccGCTAATCTTCTTGAACAGCCGCCAGCCGCTCA Ccatctgttgtcacttactgtacaagcaaagcaatattgtcactgc)	Fasmac	N/A
ORF6-HiBiT-Fw (CTGTTCAAGAAGATTAGCgggagttctggctttcatct cgttgactttcaggttactatagcagagatattactaattat)	Fasmac	N/A
Recombinant DNA		
pCSII-CoV-2-G1	This paper	N/A
pCSII-CoV-2-G2	This paper	N/A
pCSII-CoV-2-G3	This paper	N/A
pCSII-CoV-2-G4	This paper	N/A
pMW-CoV-2-G5	This paper	N/A
pMW-CoV-2-G6	This paper	N/A
pCSII-CoV-2-G7	This paper	N/A
pCSII-CoV-2-G8	This paper	N/A
pCSII-CoV-2-G9	This paper	N/A
pCSII-CoV-2-G10	This paper	N/A
pMW-CoV-2-UTRlinker	This paper	N/A
pCSII-CoV-2-G10-sfGFP	This paper	N/A
pCAGGS-CoV-2-N	This paper	N/A

RESOURCE AVAILABILITY

Lead contact
Further information and requests for resources and reagents should be directed to the two Lead Contacts, [Takasuke Fukuhara (fukut@pop.med.hokudai.ac.jp) or Yoshiharu Matsuura (matsuura@biken.osaka-u.ac.jp)].

Materials availability
All unique materials generated in this study are available from either of the two Lead contacts [Takasuke Fukuhara (fukut@pop.med.hokudai.ac.jp) or Yoshiharu Matsuura (matsuura@biken.osaka-u.ac.jp)] with a completed Materials Transfer Agreement.

Data code and availability
This study did not generate any unique datasets or code.

EXPERIMENTAL MODEL AND SUBJECT DETAILS

SARS-CoV-2 strain SARS-CoV-2/Hu/DP/Kng/19-020 was kindly provided by Dr. Sakuragi at the Kanagawa Prefectural Institute of Public Health. All viruses were initially amplified in Vero E6 cells and the culture supernatants were harvested and stored at -80°C until use. BHK-21 cells and Vero E6 cells were maintained in high-glucose Dulbecco's Modified Eagle Medium (DMEM) (Nacalai Tesque) containing 10% fetal bovine serum (FBS) (Sigma), 100 units/ml penicillin and 100 μg/ml streptomycin (P/S) (Sigma). TMPRSS2-expressing Vero E6 (VeroE6/TMPRSS2) cells were obtained from the Japanese Collection of Research Bioresources Cell Bank (JCRB1819), and maintained in DMEM containing 10% FBS and G418 (Nacalai Tesque). IFNAR1-deficient HEK293 cells, in which human ACE2 and TMPRSS2 are induced by tetracycline, were established and designated as HEK293-3P6C33 cells. In brief, ACE2 carboxyl terminally tagged with BFP followed by IRES-TMPRSS2 was constructed under a tetracycline-responsible promoter in a piggyback-based vector (Yusa et al., 2009) (kindly provided from Welcome Trust Sanger Institute). EF-1alpha-driven rtTA-P2A-bsd was also inserted into this vector. Then, this plasmid was co-transfected with a transposase-expression vector, pCMV-hyPBase (Yusa et al., 2011) (kindly provided from Welcome Trust Sanger Institute), into HEK293 cells, whose IFNAR1 had been knocked out using a CRISPR/Cas9 system. The HEK293-3P6C33 cells were maintained in DMEM containing 10% FBS and Blasticidin (solution) (10 μg/ml) (Invivogen), and the exogenous expression of ACE2 and TMPRSS2 was induced by addition of doxycycline hydrochloride (1 μg/ml) (Sigma). All the above cells were cultured at 37°C under 5% CO_2. All experiments involving SARS-CoV-2 were performed in biosafety level-3 laboratories, following the standard biosafety protocols approved by the Research institute for Microbial Diseases at Osaka University.

METHOD DETAILS

RNA extraction, cDNA synthesis, and determination of nucleotide sequences of the full-length SARS-CoV-2 genome
Total RNA was extracted from the supernatants of SARS-CoV-2-infected cells by using a PureLink RNA Mini Kit (Invitrogen). Thereafter, first-strand cDNA was synthesized by using a PrimeScript RT reagent kit (Perfect Real Time) (TaKaRa Bio) with random hexamer primers and extracted RNA, according to the manufacturer's protocols. To determine the nucleotide sequences of full-length SARS-CoV-2, a total of 10 gene fragments (G1–G10), which are up to 4,000 base pairs in length and cover the entire SARS-CoV-2 sequence, were amplified with synthesized cDNA, specific primer sets for SARS-CoV-2 and PrimeSTAR GXL DNA polymerase (TaKaRa Bio). The 5′ termini of RNA were amplified by using the 5′RACE System for Rapid Amplification of cDNA Ends, Version 2.0 (Thermo Fisher Scientific) with specific primers (CoV-2-Race1 and CoV-2-Race2) as previously described (Li et al., 2005). Then, the amplified products were directly sequenced in both directions by using the ABI PRISM 3130 Genetic Analyzer (Applied Biosystems) with specific primers.

Plasmids
A total of 10 SARS-CoV-2 (HuDPKng19-020) cDNA fragments (G1–G10) were amplified by PrimeSTAR GXL DNA polymerase and cloned into plasmids. SARS-CoV-2 fragments (G1, G2, G3, G4, G7, G8, G9 and G10) were cloned into the lentiviral vector pCSII-EF-RfA (pCSII-CoV-2-G1, -G2, -G3, -G4, -G7, -G8, -G9 and -G10), and other fragments (G5 and G6) were cloned into the pMW119 vector (pMW-CoV-2-G5 and -G6). A UTR linker for SARS-CoV-2 was also generated using the pMW119 vector, which encodes sequences of the 3′ 43 nt of SARS-CoV-2, BGH polyA signal, HDVr, CMV promoter and the 5′ 25 nt of SARS-CoV-2 (pMW-CoV-2-UTRlinker). To distinguish between the recombinant viruses and the original virus, two silent mutations, A7,486T and T7,489A, were introduced into pCSII-CoV-2-G4 as genetic markers by site-directed mutagenesis. To generate reporter viruses possessing the sfGFP gene, the nucleotide sequences of 27,433–27,675 in the ORF7 region in pCSII-CoV-2-G10 were replaced with the sfGFP gene as previously described (Thi Nhu Thao et al., 2020) by site-directed mutagenesis. The resulting vectors were designated as pCSII-CoV-2-G10-sfGFP. A plasmid expressing the SARS-CoV-2 nucleocapsid was constructed by inserting the cDNA of the nucleocapsid into pCAGGS (pCAGGS-CoV-2-N). Sequences of all the inserted DNAs were confirmed by sequencing (ABI PRISM 3130 Genetic Analyzer).

CPER reaction

SARS-CoV-2 recombinants were generated by CPER as described previously (Setoh et al., 2017), with some modifications. To amplify all the cDNA fragments having complementary ends with a 25- to 452-nucleotide overlap for CPER, plasmids encoding SARS-CoV-2 gene fragments (G1–G10) and UTR linker were used as templates. The specific primers used to amplify DNA fragments (F1–F10 and the UTR linker) are described in the Key Resources Table (CoV-2-F1-Fw to CoV-2-Linker-Rv). Then, the DNA fragments of F9 and F10 were connected before CPER by overlap PCR with a primer set (CoV-2-F9-Fw and CoV-2-F10-Rv). By using equimolar amounts (0.1 pmol each) of the resulting 10 DNA fragments (F1 to F8, F9/10 and the UTR linker) and 2 μL of PrimeStar GXL DNA polymerase, CPER was performed within 50 μL reaction volumes. The cycling conditions of CPER were as follows: condition 1 (an initial 2 minutes of denaturation at 98°C; 20 cycles of 10 s at 98°C, 15 s at 55°C, and 25 minutes at 68°C; and a final extension for 25 minutes at 68°C), condition 2 (an initial 2 minutes of denaturation at 98°C; 35 cycles of 10 s at 98°C and 15 minutes at 68°C; and a final extension for 15 minutes at 68°C), or condition 3 (an initial 2 minutes of denaturation at 98°C; 35 cycles of 10 s at 98°C, 15 s at 55°C, and 15 minutes at 68°C; and a final extension for 15 minutes at 68°C).

The infectious clones of SARS-CoV-2 carrying sfGFP were also assembled by CPER using pCSII-CoV-2-G10-sfGFP as templates to acquire DNA fragment F10. The HiBiT recombinant SARS-CoV-2 was also generated by CPER. The HiBiT sequence (VSGWRLFKKIS) and a linker sequence (GSSG) were inserted in the N terminus of the ORF6 sequence by overlap PCR using DNA fragment F9 and a specific overlap primer set (ORF6-HiBiT-Rv and ORF6-HiBiT-Fw) and fragment F9-amplifying primer set (CoV-2-F9-Fw and CoV-F9-Rv). Thereafter, CPER was conducted using the resulting fragment F9 containing the HiBiT gene.

Transfection

The CPER products (25 μL out of a 50 μL reaction volume) without purification were transfected into HEK293-3P6C33 cells or BHK-21 cells with Trans IT LT-1 (Mirus), following the manufacturer's protocols. At 6 hours post-transfection, the culture supernatants of HEK293-3P6C33 cells were replaced with DMEM containing 2% FBS and doxycycline hydrochloride (1 μg/ml), and BHK-21 cells were overlaid by VeroE6/TMPRSS2 cells.

Titration and growth kinetics

The infectious titers in the culture supernatants were determined by the 50% tissue culture infective doses (TCID$_{50}$). The culture supernatants of cells were inoculated onto VeroE6/TMPRSS2 cells in 96-well plates after ten-fold serial dilution with DMEM containing 2% FBS, and the infectious titers were determined at 72 hours post-infection (hpi). For growth kinetics, SARS-CoV-2 was inoculated into VeroE6/TMPRSS2 cells in 6-well plates at a multiplicity of infection (MOI) of 0.001 or 0.01 and the culture supernatants were replaced with new media at 1 hpi and incubated for 48 hours. The infectious titers in the culture supernatants of cells collected at 12, 24, 36 and 48 hpi were determined.

Northern blotting

Total RNAs were extracted from cells infected with the WT or recombinant SARS-CoV-2 and subjected to Northern blot analysis as previously described (Xie et al., 2020). A digoxigenin (DIG)-labeled random-primed probe, corresponding to 28,999 to 29,573 of the SARS-CoV-2 genome, was generated by using a DIG RNA Labeling kit (SP6/T7) (Roche), and utilized to detect viral mRNAs. The RNAs were washed with the DIG luminescent detection kit (Roche) and visualized with CDP-Star Chemiluminescent Substrate (Roche), according to the manufacturer's protocols.

HiBiT luciferase assay

SARS-CoV-2 infected cells were collected at the indicated time points and subjected to luciferase assay. Luciferase activity was measured by using a Nano-Glo HiBiT Lytic assay system (Promega), following the manufacturer's protocols. In brief, the HiBiT assay was conducted by adding Nano-Glo substrate and LgBiT protein into the lysates of cells infected with viruses, and then measuring the luciferase activities with a luminometer.

QUANTIFICATION AND STATISTICAL ANALYSIS

All assays were performed independently at least 2 times. The data were expressed as means ± SD. Statistical significance was determined by the two-tailed Student's t test. P-values < 0.05 were considered significant and indicated by a single asterisk (*).

Supplemental information

Establishment of a reverse genetics system

for SARS-CoV-2 using circular

polymerase extension reaction

Shiho Torii, Chikako Ono, Rigel Suzuki, Yuhei Morioka, Itsuki Anzai, Yuzy Fauzyah, Yusuke Maeda, Wataru Kamitani, Takasuke Fukuhara, and Yoshiharu Matsuura
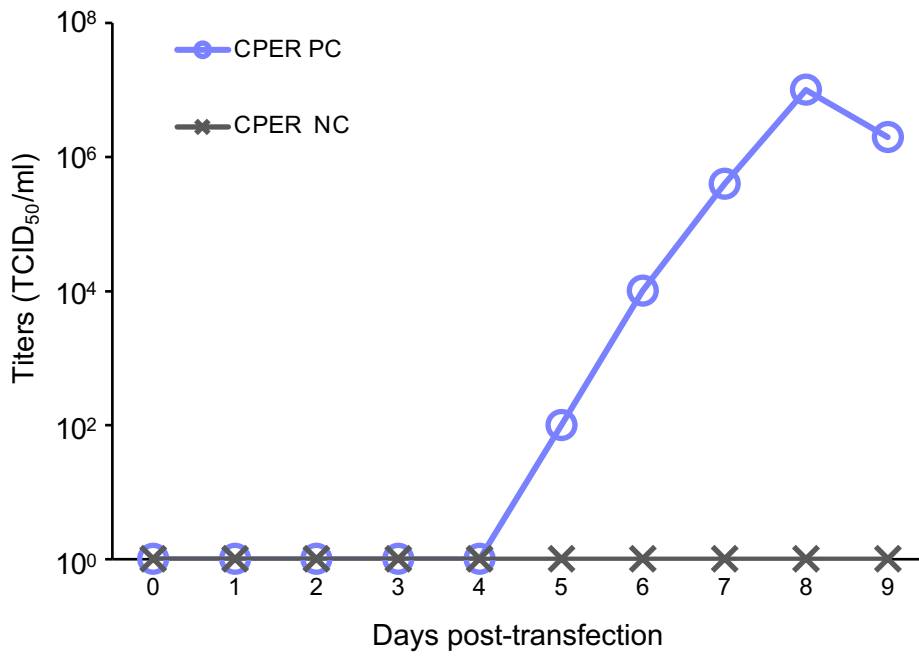
Figure S1. Production of recombinant SARS-CoV-2. Figure S1 is related to Figure 1A.
CPER products were transfected into HEK293-3P6C33 cells (CPER PC) and infectious titers
in the culture supernatants were measured at the indicated time points. As a negative control,
the CPER product obtained without fragment F9/10 was transfected into cells (CPER NC).
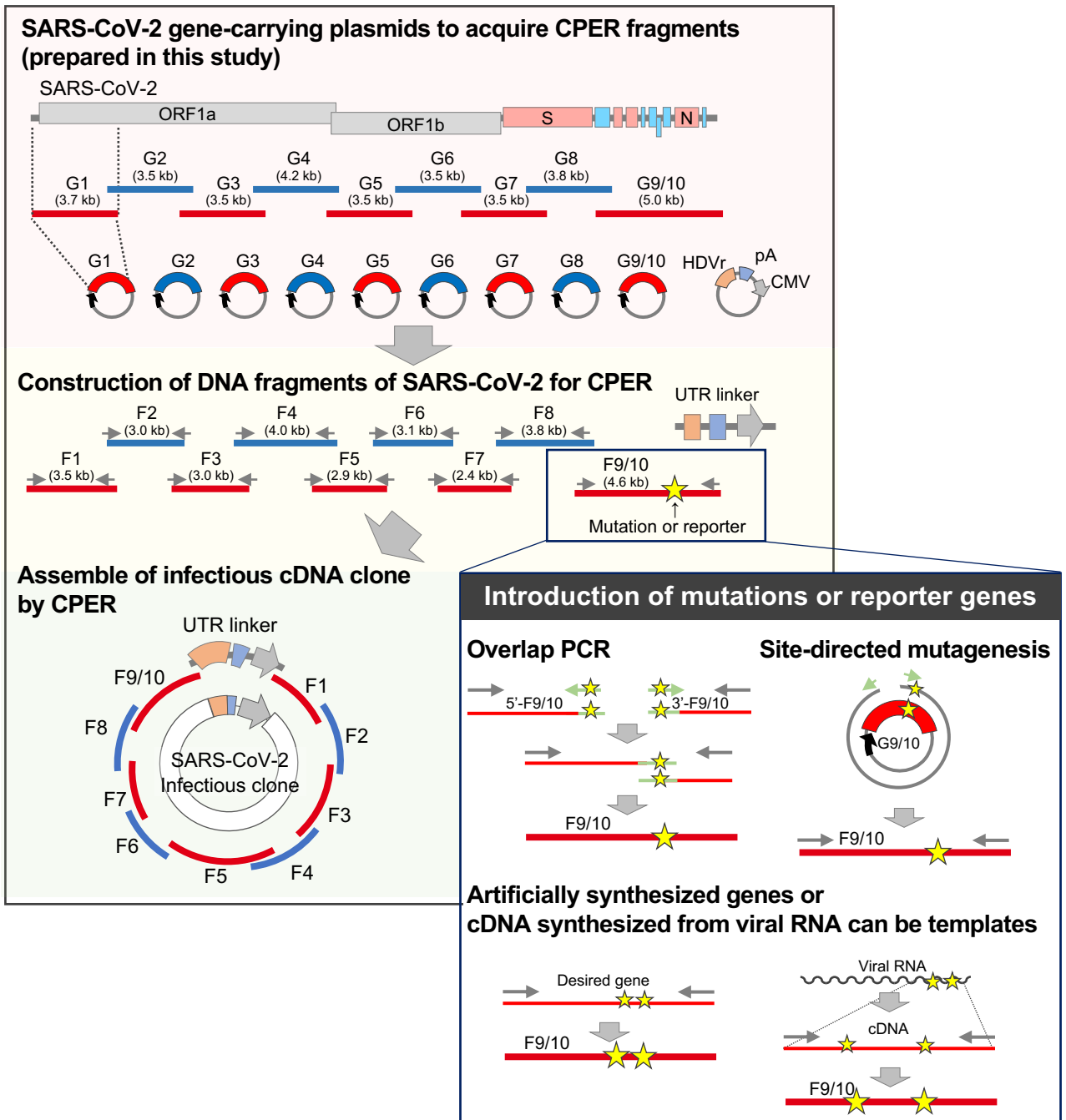
Fig. S1 Torii et al.

Figure S2. Workflow to generate infectious cDNA clone for SARS-CoV-2 with desirable mutations or reporters. Figure S2 is related to Figure 2.
By using DNA fragments and overlapping primers, which possess mutations or reporter genes, mutation can be introduced. By site-directed mutagenesis using SARS-CoV-2 gene-encoding plasmids, mutations can also be introduced. Using artificially synthesized gene fragments with mutations, multiple mutations can be inserted more quickly. In addition, reverse-transcribed cDNA from viral RNA can be used as templates for amplification of DNA fragments of SARS-CoV-2.
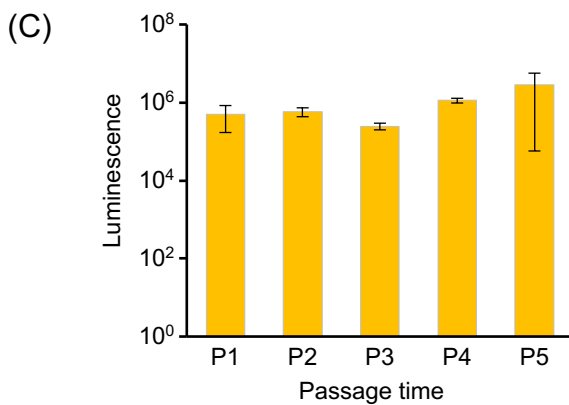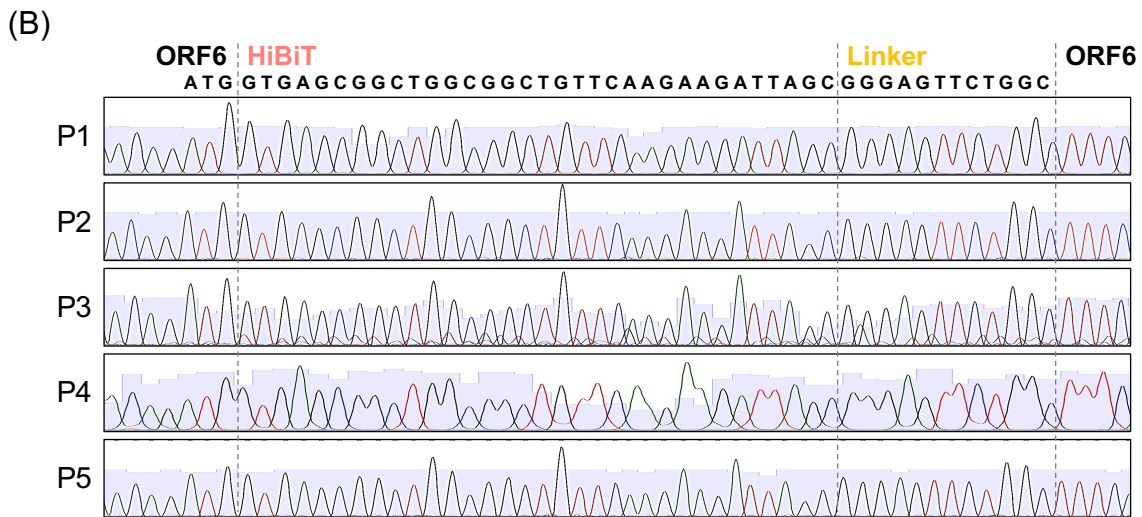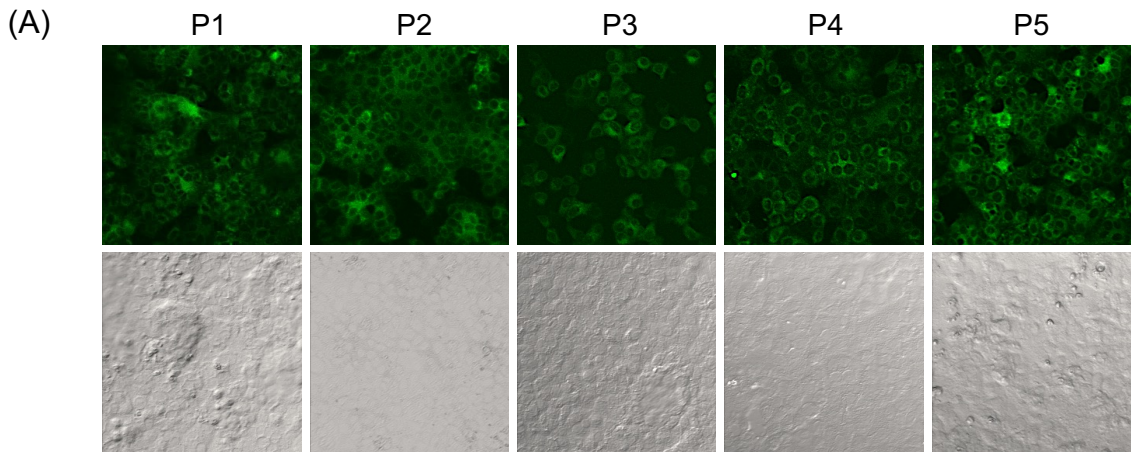
Fig. S2 Torii et al.

Figure S3. Stability of reporter genes in recombinant SARS-CoV-2 engineered by CPER. Figure S3 is related to Figure 2A-E.
(A) GFP viruses serially passaged for five times (P1-P5) were infected with VeroE6/TMPRSS2 cells at an MOI of 0.01 and the fluorescent signals in cells were observed at 24 hpi. (B) HiBiT viruses were serially passaged for five rounds (P1-P5), and the sequence of HiBiT and a linker inserted into the ORF6 of each virus was determined. (C) HiBiT viruses (P1-P5) were inoculated into VeroE6/TMPRSS2 cells at an MOI of 0.01 and luciferase activities were determined at 24 hpi.

Fig. S3 Torii et al.